

Degree of Skin Barrier Disruption Affects Lipid Organization in Regenerated Stratum Corneum

Tineke BERKERS, Dani VISSCHER, Gert S. GOORIS and Joke A. BOUWSTRA

Department of Drug Delivery Technology, Cluster BioTherapeutics, Leiden Academic Centre for Drug Research, Leiden University, Leiden, The Netherlands

Previously, a skin barrier repair model was developed to examine the effect of formulations on the lipid properties of compromised skin. In this model, the lipid organization mimics that of several skin diseases with impaired skin barrier and less dense lateral lipid organization. In addition, parakeratosis was occasionally observed. The present study investigated whether the extent of initial barrier disruption affects lipid organization and parakeratosis in regenerated stratum corneum. After barrier disruption and stratum corneum regeneration the fraction of lipids adopting a less dense lateral organization gradually increased with increasing degree of barrier disruption. Only when 75% of the stratum corneum was removed, were parakeratosis and a change in lamellar organization observed. This demonstrates the possibility of using the skin barrier repair model to study the effects of formulations on compromised skin in which the presence of parakeratosis and lipid organization can be modified by the extent of barrier disruption.

Key words: skin barrier repair; parakeratosis; lateral lipid organization; lamellar lipid organization; stratum corneum; skin model.

Accepted Dec 14, 2017; Epub ahead of print Dec 15, 2017

Acta Derm Venereol 2018; 98: 421–427.

Corr: Joke A. Bouwstra, Department of Drug Delivery Technology, Cluster BioTherapeutics, Leiden Academic Centre for Drug Research, Einsteinweg 55, NL-2333 CC Leiden, The Netherlands. E-mail: bouwstra@lacdr.leidenuniv.nl

The skin barrier function is located in the uppermost layer of the epidermis, the stratum corneum (SC). This layer consists of corneocytes embedded in a lipid matrix (1). The lipids form 2 crystalline lamellar phases with repeat distances of 13 nm (long periodicity phase, LPP) and 6 nm (short periodicity phase, SPP), see Fig. 1 (2–4). Within the lipid lamellae, the lipids mainly adopt a dense orthorhombic lateral packing in healthy skin (5–8). In several skin diseases, the barrier function is affected, e.g. atopic dermatitis, lamellar ichthyosis, Netherton syndrome, and psoriasis (9). The reduced barrier function is characterized by, for example, a higher fraction of SC lipids that adopts a hexagonal lateral packing compared with healthy skin (10). The change in barrier function in several skin diseases depends on the severity of the disease (9–11).

Recently, a human skin barrier repair model was developed that can be used to study the interactions of topical

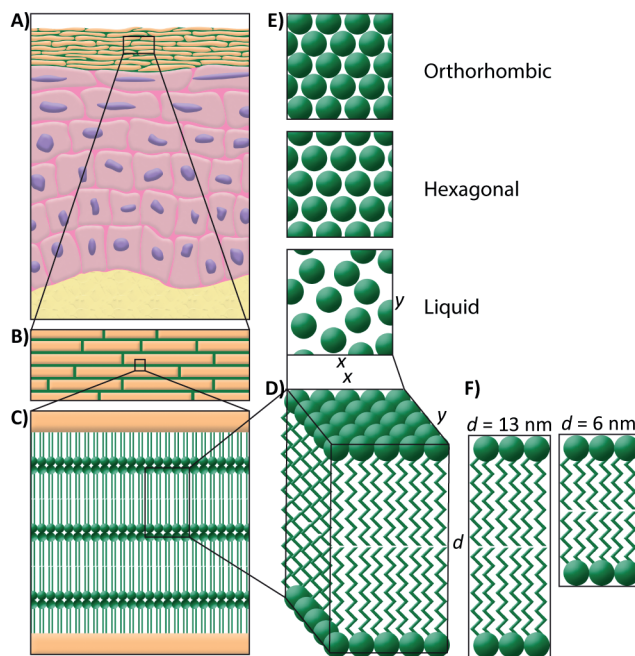


Fig. 1. Lipid organization in the stratum corneum. (A) Schematic overview of the skin. (B) A brick and mortar structure is mimicking the corneocytes embedded in the lipid matrix. (C) In between the corneocytes, the lipids are stacked in lamellae. (D) Detail of the lipid lamellae. (E) Perpendicular to the lamellae, the lipids are organized in a lateral packing. This can be either orthorhombic, hexagonal, or liquid (top view). (F) The lipid lamellae are stacked on top of each other with a repeat distance (d) of either 13 nm (long periodicity phase) or 6 nm (short periodicity phase).

formulations with the SC during skin barrier repair (12). This model is referred to as the SkinBaR model and exhibits several characteristics of the lipid composition and organization in SC of diseased skin, such as Netherton syndrome, lamellar ichthyosis, and atopic dermatitis. In this model, the SC is removed by stripping *ex vivo* human skin and regenerated during a culture period of 8 days. In our previous studies, nuclei were occasionally observed in the regenerated SC after culturing, which is known as parakeratosis. Parakeratosis is also observed in several skin diseases with a disturbed barrier (13), wound healing (14), and after tape-stripping *in vivo* (15). It is caused by abnormal keratinocyte maturation. We hypothesize that the degree of barrier disruption influences the rate at which the barrier is repaired and may therefore be associated with the presence of parakeratosis and the extent the lipid organization in the SC lipid matrix changes, mimicking more closely the lipid organization in SC of diseased skin. If this is the case, the SkinBaR model could

be used to study the effects of barrier repair formulations on various levels of altered lipid organization, mimicking several aspects of the lipid organization in diseased skin. The formulations can be applied during or after barrier regeneration (16).

The aim of this study was to induce several degrees of barrier disruption by stripping *ex vivo* human skin and regenerating the SC during culture. We intended to mimic multiple levels of skin disease severity as analysed by the morphology and lateral and lamellar lipid organization, which are indicative for skin barrier function.

METHODS

Chemicals

Cyanoacrylate (Bison, Goes, the Netherlands) was bought in a local shop. Xylene was purchased from Biosolve (Valkenswaard, the Netherlands), 4% buffered formaldehyde was acquired from Added Pharma (Oss, the Netherlands), paraffin, haematoxylin, and eosin were obtained from Klinipath (Duiven, the Netherlands). DMEM, Ham's F12, and penicillin/streptomycin were purchased from Fisher Scientific (Waltham, MA, USA). Bovine serum albumin, sodium bromide, ethanol, acetone, trypsin, trypsin inhibitor, selenious acid, hydrocortisone, isoproterenol, L-carnitine, L-serine, insulin, α -tocopherol acetate, vitamin C, arachidonic acid, linoleic acid, and palmitic acid were purchased from Sigma-Aldrich (Zwijndrecht, the Netherlands).

Stripping and culturing of *ex vivo* skin

Human abdomen or mamma skin from 3 donors (age 20, 30, and 67 years) was obtained after abdominoplasty or breast reduction, from a local hospital, after written informed consent, and was used within 12 h after cosmetic surgery. Subcutaneous fat was removed with a scalpel, and the skin was wiped with 70% ethanol and Millipore water. Subsequently, the skin was dermatomed to a thickness of 600 μ m (D80 Dermatome, Humeca, Borne, the Netherlands), punched in circles (ϕ =26 mm), clamped in a custom-made device, and stripped with preheated cyanoacrylate on a preheated metal cylinder, as described previously (12). SC was stripped by removing the cylinder in one stroke. The stripping procedure was repeated to remove either 25%, 50% or 75% of the SC. After 75% of the SC was removed the skin appeared shiny. Typically, 6–8 strips were needed to reach a shiny appearance of the whole sample, varying between skin donors. Cultured non-stripped (0%) skin and native skin (e.g. non-stripped and not cultured) were used as control. Per donor, the different conditions were cultured in duplicate.

The stripped *ex vivo* skin was cultured at the air-liquid interface for 8 days in a deep 6-well culturing plate (Organogenesis, Canton, MA, USA), as described previously (12). The samples were either cryofixed, paraffin embedded, or SC was isolated.

Isolation of stratum corneum

SC was isolated from the (cultured) skin by trypsin digestion. The skin was placed in 0.1% trypsin solution in phosphate-buffered saline (PBS) and kept overnight at 4°C, followed by 1 h at 37°C. Trypsin is a proteolytic enzyme which is used to separate SC from the epidermis (17). SC was peeled off, washed in 0.1% trypsin inhibitor, and twice in Millipore water. SC sheets were stored over silica gel under argon until use. SC was used for either infrared spectroscopy measurements or X-ray diffraction measurements.

Safranin-O red and haematoxylin and eosin staining

To examine the number of corneocyte layers 5 μ m cryofixed sections were stained with 1% (w/v) Safranin-O solution for 1 min followed by 20 min incubation in 2% (w/v) KOH solution. Haematoxylin and eosin (HE) staining was performed on 5 μ m paraffin sections to examine the morphology. After Safranin-O and HE staining, at least 3 light microscopy images were taken per culture condition at 20 \times and 63 \times magnification.

Fourier transform infrared spectroscopy

Fourier transform infrared (FTIR) spectroscopy was used to examine the lateral lipid packing of isolated SC samples as a function of temperature (0–90°C). The samples were placed over a 27% NaBr solution in D2O for 24 h at room temperature, reaching a final hydration level of approximately 20% in the SC, and sandwiched between 2 AgBr-windows. Spectra were obtained using a Varian 670-IR FTIR spectrometer (Agilent Technologies, Santa Clara, CA, USA), as described previously (16).

The onset temperature of the ordered-disordered transition was obtained from the peak positions of the CH₂ symmetrical stretching vibrations in the FTIR spectra. Peak positions were plotted as a function of temperature. The intercept of 2 regression lines fitted to the linear parts of the graph was calculated, which describes the onset transition temperature, as described previously (16).

Small-angle X-ray diffraction

Small-angle X-ray diffraction (SAXD) was used to examine the lamellar organization of the SC lipids. Measurements were performed at the European Synchrotron Radiation Facility (Grenoble, France) using the Dutch-Belgian beamline (station BM26B). Twenty-four hours prior to the measurements, SC samples were hydrated over a 27% NaBr solution at room temperature, reaching a hydration level of approximately 20%. A custom-made sample holder was used to orientate the samples parallel to the X-ray beam. Diffraction data was collected at room temperature on a Pilatus 1M detector for a period of 5 or 10 min, as described earlier (18). The scattering vector (q) was calculated using the scattering angle (Θ) and the wavelength (λ) by $q=4\pi \sin \Theta/\lambda$. The spacing of the lamellar phase can be calculated from the position of the peak maxima (q) using $2\pi/q$.

Statistical analysis

One-way ANOVA with *post hoc* correction for multiple comparisons or with a *post hoc* trend test was used to analyse the data using GraphPad Prism 7 (San Diego, CA, USA). All differences are described relative to native human skin.

RESULTS

Human skin cultured after various degrees of barrier disruption results in complete regeneration of the stratum corneum

After staining with safranin-O, the number of corneocyte layers was determined for at least 3 different spots per image and at least 3 images were taken per culturing condition for each skin donor. Per condition, the results of the 3 donors were pooled. Native human skin showed 11.0 ± 4.0 (mean \pm standard deviation (SD)) corneocyte

layers, whereas after removing the SC until the skin surface appeared shiny 3.1 ± 2.8 SC cell layers remained on the viable epidermis, meaning that about 75% of the corneocyte layers was removed. The number of strips needed to remove 75% of the SC was reduced to three-quarters and half in order to obtain less stripped skin. This resulted in skin with either 5.0 ± 3.4 (=50% stripped) or 7.7 ± 4.4 (=25% stripped) remaining corneocyte layers on the viable epidermis (Fig. 2A). All stripped samples had a significant lower number of corneocyte layers than the native SC ($p < 0.001$). A *post-hoc* test showed that there is a linear trend with decreasing number of corneocyte layers for the samples prior to culture (slope:

-2.6 , $p < 0.0001$). After the 8-day culturing period, the number of corneocyte layers in the regenerated SC is significantly increased to 10.8 ± 3.6 , 10.3 ± 2.6 , and 11.2 ± 3.1 , for 75%, 50%, and 25% stripped SC, respectively, which is comparable to the number of layers in native human skin before stripping.

Parakeratosis is visible when the majority of the stratum corneum is removed

The morphology of the cultured skin sections was visualized using HE staining. Staining revealed that after removing 75% of the SC and subsequent culturing, prominent parakeratosis is observed (Fig. 2E, *arrows*), mainly in the top layers of the regenerated SC. Furthermore, spongiosis with an irregular keratinocyte distribution in the epidermis was observed in skin with SC that was regenerated after 75% of the SC was removed. After 50% or 25% of the SC was removed, the regenerated SC did not exhibit parakeratosis or major differences in morphology.

Lateral lipid organization changes gradually with number of removed corneocyte layers

The lipid organization of the stripped and regenerated SC was examined and compared with native SC. The lateral lipid packing was examined using the CH_2 rocking vibrations in the FTIR spectra in a temperature range between 0°C and 90°C . A hexagonal lateral lipid packing is characterized by a single contour positioned at a wave-number of 719 cm^{-1} , while an orthorhombic packing is characterized by a doublet positioned at 719 and 730 cm^{-1} . All spectra were scaled at the difference between the absorption at 719 cm^{-1} (peak position) and the absorption at 715 cm^{-1} (base). This difference in absorption was kept constant in all spectra. In this way relative peak heights of the peak at approximately 730 cm^{-1} could be compared between samples.

Fig. 3 shows representative FTIR spectra of 1 donor. In native SC 2 strong contours were observed at 719 and 730 cm^{-1} at 0°C (Fig. 3A), indicating that the lipids adopt an orthorhombic lateral lipid packing. The contour positioned at 730 cm^{-1} started to decrease in intensity at approximately 34°C and disappeared at approximately 48°C , indicating a phase transition from an orthorhombic to a hexagonal lateral lipid packing. The intensity of the peak at 730 cm^{-1} at 0°C gradually decreased when 25% to 50% and 75% of SC was removed before culturing. When increasing the temperature, the peak at 730 cm^{-1} disappeared between 30°C and 48°C (25% of SC was stripped), and 20°C and 36°C (50% of SC was stripped) in the FTIR spectra of regenerated SC. After removing 75% of the corneocyte layers and regeneration of the SC, the orthorhombic to hexagonal transition occurred between 8°C and 30°C , as monitored by the disappearance of the 730 cm^{-1} in the corresponding FTIR spectrum.

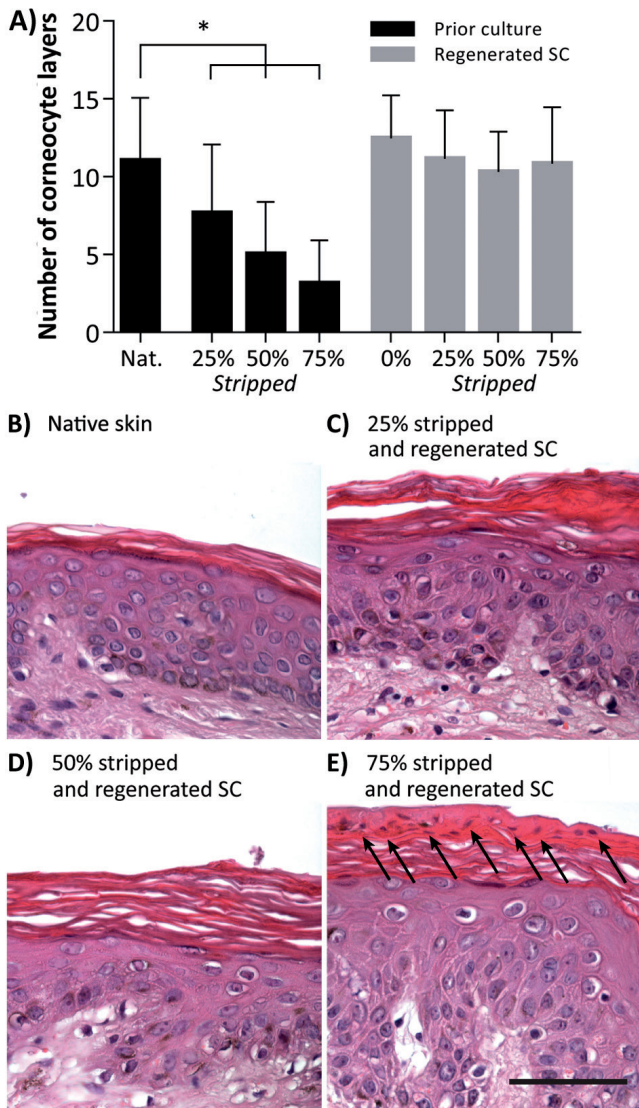


Fig. 2. Number of corneocyte layers and morphology. (A) The number of layers in native (Nat.) stratum corneum (SC), stripped SC, and regenerated SC after culturing. Bars represent mean \pm standard deviation. Morphology of (B) native skin, and (C-E) stripped and cultured skin with regenerated SC. SC was stripped away by 25%, 50%, and 75%, respectively. * $p < 0.001$ (analysis of variance; ANOVA), arrows: parakeratosis, scale bar: $50\text{ }\mu\text{m}$.

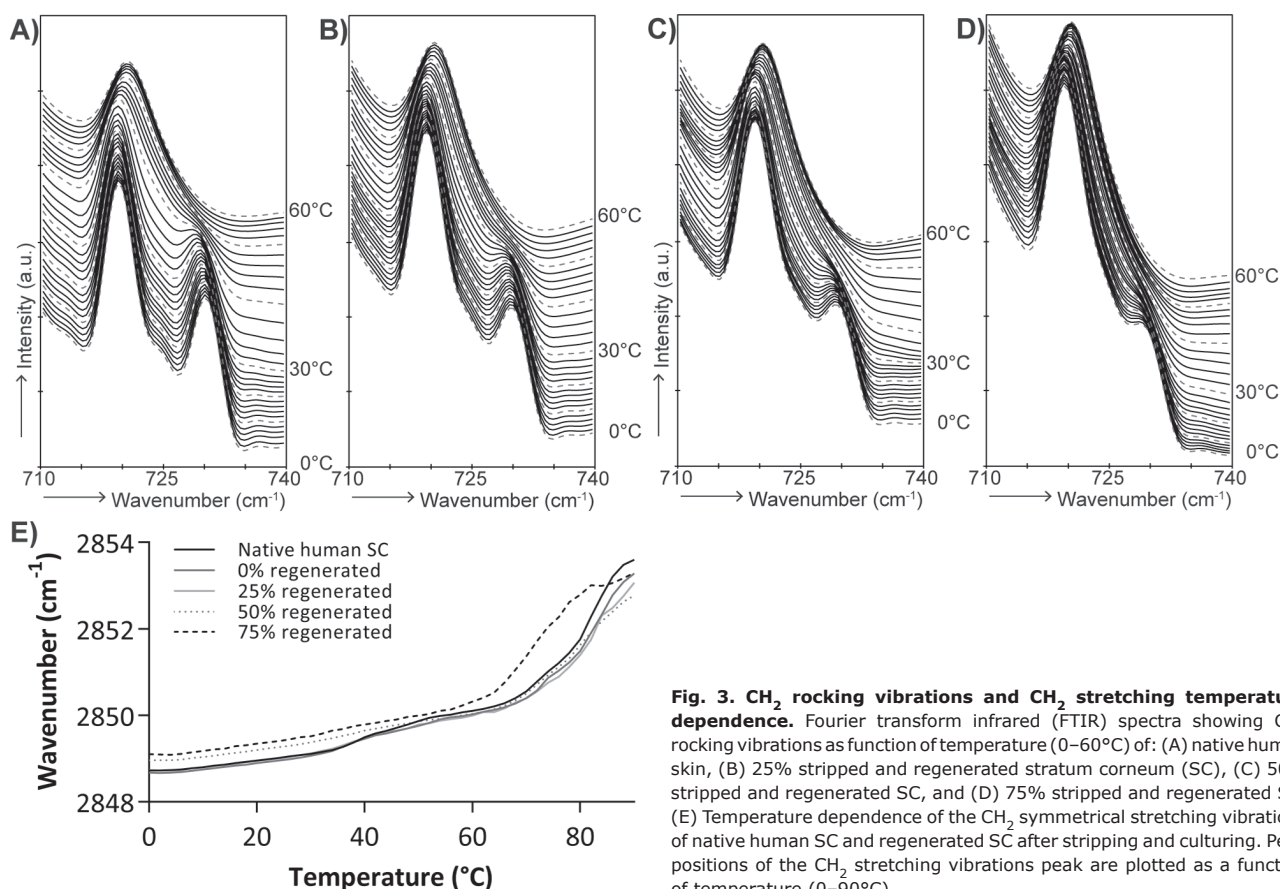


Fig. 3. CH₂ rocking vibrations and CH₂ stretching temperature dependence. Fourier transform infrared (FTIR) spectra showing CH₂ rocking vibrations as function of temperature (0–60°C) of: (A) native human skin, (B) 25% stripped and regenerated stratum corneum (SC), (C) 50% stripped and regenerated SC, and (D) 75% stripped and regenerated SC. (E) Temperature dependence of the CH₂ symmetrical stretching vibrations of native human SC and regenerated SC after stripping and culturing. Peak positions of the CH₂ stretching vibrations peak are plotted as a function of temperature (0–90°C).

Lipid ordering is only affected when significant amount of stratum corneum is removed

The conformational ordering of the lipids was examined using the thermotropic behaviour of the CH₂ symmetrical stretching vibrations in the FTIR spectrum in a temperature range of 0–90°C. Fully extended lipid chains show high conformational ordering, which is characterized by a CH₂ stretching vibration peak position at wavenumbers below 2,850 cm⁻¹. When lipids have a high conformational disordering, e.g. when lipids are in the liquid state, the peak position is shifted to wavenumbers higher than 2,852 cm⁻¹. The onset transition temperature was determined as described above.

The CH₂ symmetrical stretching vibrations obtained from representative data of 1 donor are plotted as a function of temperature in Fig. 3E. The wave-number at 10°C and the onset transition temperatures are mean values of the spectra of the 3 donors. At 10°C, a wave-number of 2,848.81 ± 0.01 cm⁻¹ (mean ± SD) was observed in native SC. The wave-numbers of cultured control skin, and after regeneration of 25% and 50% of the SC were comparable to native SC ($p=0.74$, $p=0.35$, and $p=0.39$, respectively). Only when 75% of the SC was removed, the wave-number at 10°C was increased to 2,849.38 ± 0.25 cm⁻¹ ($p=0.04$). This indicates that, even at low temperatures, the lipid ordering of the regenerated SC is affected.

Furthermore, the stretching vibrations are used to compare the onset transition temperatures of the ordered-disordered phase transition. For native SC the onset transition temperature was 72.5 ± 3.6°C (mean ± SD). Furthermore, at approximately 30–40°C, a small shift in wave-number is observed, indicating an orthorhombic to hexagonal transition. Lipids in the SC of cultured control skin (0% of SC was stripped) showed similar temperature dependence as native SC with a transition temperature of 68.9 ± 4.7°C. After regeneration of the SC after 25% or 50% of the SC was stripped, the onset temperatures of the ordered-disordered phase transition were 68.9 ± 2.9°C and 67.9 ± 1.3°C, respectively. These onset transition temperatures were not statistically significantly different from that of native SC. However, SC regeneration after 75% of the SC was removed, resulting in a different temperature dependence of the CH₂ stretching vibrations. The onset of the ordered-disordered phase transition took place at a statistically significant lower temperature of 62.9 ± 2.1°C ($p=0.01$). This is apparent from the line in Fig. 3E, which is shifted to the left and increases to higher wave-numbers at lower temperatures. Furthermore, the small shift in wave-number at approximately 30–40°C was not observed in regenerated SC after 50% or 75% of the SC was stripped.

The lamellar repeat distance decreases only after removing most of the stratum corneum

The lamellar organization in the lipid matrix was examined using SAXD. Fig. 4 shows SAXD patterns of a representative donor of native SC and SC that was regenerated after stripping and culturing. Two weak diffraction peaks (indicated by I and III) and 1 strong peak (indicated by II) can be observed. The LPP contributes to all 3 peaks, whereas the SPP only contributes to peak II. The peak corresponding to phase separated cholesterol is marked by an asterisk. The peak position (q) of the main peak (II) was used to examine whether a difference in lamellar spacing was induced by SC disruption. The spacing of the lipids in the stripped and regenerated SC was compared with the spacing of native SC of the same donor. In this way, a mean difference was obtained. The spacing in native SC was 6.3 ± 0.1 nm (mean \pm SD). The difference in spacing was 0.05 nm for the SC of the cultured control sample (0% of SC was stripped) and for regenerated SC after 25% or 50% of the SC was stripped this difference was -0.06 nm. None of these changes were statistically different. However, when SC was regenerated after 75% of the SC was removed, the difference in spacing was -0.23 nm, which was statistically significant different from native SC ($p=0.001$). Furthermore, the intensity of diffraction peaks I and III decreased substantially, indicating a reduction in the presence of the LPP. In addition, a shoulder appears close to the position of peak II at a q -value of approximately 1.3 nm $^{-1}$.

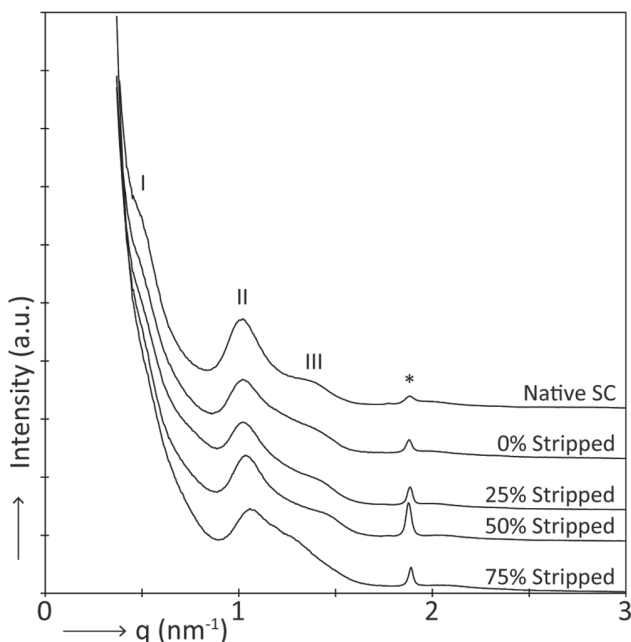


Fig. 4. A typical example of small angle X-ray diffraction (SAXD) patterns of native stratum corneum (SC) and regenerated SC after stripping and culturing. The peak positions (q) are indicative for the spacing of the lipid lamellae. The 1st, 2nd, and 3rd order peaks of the long periodicity phase (LPP) are labelled I, II, and III, respectively. The first order of the short periodicity phase (SPP) also contributes to peak II. *Phase separated cholesterol.

DISCUSSION

This study showed that, in regenerated SC of the SkinBaR model, on demand one can gradually decrease the fraction of lipids adopting a dense orthorhombic lateral packing by varying the initial degree of barrier disruption. The obtained changes in lipid lateral packing compared with native SC are very similar to that observed in SC of several inflammatory skin diseases (9–11). These results indicate that the SkinBaR model can be used to study skin barrier repair formulations that aim to normalize the SC lipid organization in diseased skin. The degree of disruption also influenced the presence of parakeratosis, as we showed that parakeratosis was present only in the examined models when 75% of the SC was removed, resulting in 3 remaining corneocyte layers before the skin started to regenerate the SC. In addition, parakeratosis was predominantly observed in the upper corneocyte layers. This strongly indicates that only during generation of the initial corneocyte layers parakeratosis is induced, probably as a rapid response to repair the skin barrier after disruption. Independent of the degree of barrier disruption, the number of corneocyte layers after 8 days of regeneration was comparable to that in SC of native skin. This indicates that the degree of disruption affects the rate of regeneration, and that the skin is still viable. Previous observations have shown that the proliferation rate, as examined by fraction of Ki-67 positively stained nuclei, immediately after SC removal was higher than the proliferation rate after a longer recovery period (12, 15). It is known that cultured skin does not desquamate and that the corneocyte layers accumulate during culture (19). However, this is believed to be of little influence on the SkinBaR model, since the non-stripped cultured SC showed a non-significant increase of only 1.4 corneocyte layers during culturing, indicating that the formation of the SC is inhibited.

When focusing on the lateral lipid organization, the lipid density, which is the fraction of lipids forming an orthorhombic lateral packing, of the regenerated SC, decreased when the degree of barrier disruption was increased. At skin temperature (32°C), in the FTIR spectrum no contour at 730 cm $^{-1}$ was observed when 75% of the SC was regenerated, demonstrating that, at this temperature, the lipids had adopted a hexagonal packing. However, when removing less corneocyte layers, the contour at 730 cm $^{-1}$ was visible as a shoulder (after 50% of SC was stripped) or as a peak (native or after 25% of SC was stripped) at 32°C. An indication of the lipid ordering is provided by the CH $_2$ stretching vibrations. When comparing these stretching vibrations of regenerated SC after 75% of SC was stripped to that of regenerated SC after less intensive disruption of SC, the onset temperature of the ordered-disordered phase transition was significantly lower and the position of the CH $_2$ vibrations at 32°C were at higher frequency. These

observations suggest a less ordered organization of the lipids in the regenerated SC after 75% SC removal, even at low temperatures. Also the lamellar organization was only affected in regenerated SC after 75% of the SC was removed. These results indicate that the lateral lipid packing is more responsive to barrier disruption than the conformational ordering and the lamellar organization.

Previously, a more abundant presence of lipids adopting a hexagonal packing has been related to a higher level of monounsaturated fatty acids (MUFAs) (20), and shorter fatty acid (FA) and ceramide (CER) chain length (21). In the SkinBaR model, both an increased level of short-chain CER and unsaturated CER were observed (22). Monounsaturated CERs are derived from a chemical linkage of a MUFA to a sphingoid base (23). The enzyme stearoyl-CoA desaturase catalyses the conversion of saturated FAs to MUFAs. In the SkinBaR model, we have demonstrated an extended stearoyl-CoA desaturase expression compared with native human skin, suggesting also an increased level of MUFAs (12).

Similar changes in lipid organization and composition have been observed in atopic dermatitis skin. In lesional and non-lesional skin of atopic dermatitis patients a higher fraction of lipids adopts a hexagonal lipid organization, which coincides with a higher fraction of MUFAs and a reduced chain length of FAs and CERs (10, 24, 25). These changes are more pronounced in lesional skin than in non-lesional skin (10). Besides atopic dermatitis, several other skin diseases are characterized by a disrupted skin barrier (9, 11). Again, the extent of barrier disruption may vary depending on the severity of the disease. This may be of influence on the effect of topically applied barrier repair formulations.

The results in this study show that the degree of barrier disruption of the SkinBaR model can be controlled and that the changes in lipid organization and the level of parakeratosis depend on the initial extent of barrier disruption. This means that, if less corneocyte layers remain before regeneration is initiated, the deviations in lateral and lamellar lipid organization compared with native SC are more substantial. This variation in the degree of deviation of the lipid organization in the SkinBaR model can be used in studying the effect of barrier repair formulations on the lipid organization. In this way the SkinBaR model can serve as a model for the lipid organization in several skin diseases in which the lipid organization deviates in a similar manner from that in native human skin. Previously, other skin models (human skin equivalents) have been used to test topical formulations (26). However, the 8-day culturing period of the SkinBaR model is less time-consuming than the culturing period of 2–3 weeks often used to generate human skin equivalents (27–29). Furthermore, it is a challenge to influence the lateral packing of the skin equivalents by modifying the culture conditions (27, 30, 31), while the lateral packing of the SkinBaR model can be adjusted

on demand. Unlike these human skin equivalents, the SkinBaR model offers the possibility to apply topical barrier repair formulations directly after several degrees of barrier disruption and to study the lamellar and lateral lipid organization of regenerated SC.

ACKNOWLEDGEMENTS

The authors thank the personnel at DUBBLE beam line (BM26) at European Synchrotron Radiation Facility in Grenoble, France for assistance during X-ray measurements. This research was financially supported by Dutch Technology Foundation TTW (grant no. 12400).

REFERENCES

1. Michaels AS, Chandrasekaran SK, Shaw JE. Drug permeation through human skin: Theory and in vitro experimental measurement. *AIChE J* 1975; 21: 985–996.
2. Groen D, Gooris GS, Bouwstra JA. New insights into the stratum corneum lipid organization by X-ray diffraction analysis. *Biophys J* 2009; 97: 2242–2249.
3. Bouwstra J, Pilgram G, Gooris G, Koerten H, Ponc M. New aspects of the skin barrier organization. *Skin Pharmacol Appl Skin Physiol* 2001; 14 Suppl 1: 52–62.
4. McIntosh TJ, Stewart ME, Downing DT. X-ray diffraction analysis of isolated skin lipids: reconstitution of intercellular lipid domains. *Biochemistry* 1996; 35: 3649–3653.
5. Pilgram GS, Engelsma-van Pelt AM, Bouwstra JA, Koerten HK. Electron diffraction provides new information on human stratum corneum lipid organization studied in relation to depth and temperature. *J Invest Dermatol* 1999; 113: 403–409.
6. Damien F, Boncheva M. The extent of orthorhombic lipid phases in the stratum corneum determines the barrier efficiency of human skin in vivo. *J Invest Dermatol* 2010; 130: 611–614.
7. Goldsmith LA, Baden HP. Uniquely oriented epidermal lipid. *Nature* 1970; 225: 1052–1053.
8. de Jager MW, Gooris GS, Dolbnya IP, Bras W, Ponc M, Bouwstra JA. The phase behaviour of skin lipid mixtures based on synthetic ceramides. *Chem Phys Lipids* 2003; 124: 123–134.
9. van Smeden J, Janssens M, Gooris GS, Bouwstra JA. The important role of stratum corneum lipids for the cutaneous barrier function. *Biochim Biophys Acta* 2014; 1841: 295–313.
10. van Smeden J, Janssens M, Kaye EC, Caspers PJ, Lavrijsen AP, Vreeken RJ, et al. The importance of free fatty acid chain length for the skin barrier function in atopic eczema patients. *Exp Dermatol* 2014; 23: 45–52.
11. Sahle FF, Gebre-Mariam T, Dobner B, Wohlrab J, Neubert RH. Skin diseases associated with the depletion of stratum corneum lipids and stratum corneum lipid substitution therapy. *Skin Pharmacol Physiol* 2015; 28: 42–55.
12. Danso MO, Berkers T, Mieremet A, Hausil F, Bouwstra JA. An ex vivo human skin model for studying skin barrier repair. *Exp Dermatol* 2015; 24: 48–54.
13. Brady SP. Parakeratosis. *J Am Acad Dermatol* 2004; 50: 77–84.
14. Usui ML, Underwood RA, Fleckman P, Olerud JE. Parakeratotic corneocytes play a unique role in human skin wound healing. *J Invest Dermatol* 2013; 133: 856–858.
15. Gerritsen MJ, van Erp PE, van Vlijmen-Willems IM, Lenders LT, van de Kerkhof PC. Repeated tape stripping of normal skin: a histological assessment and comparison with events seen in psoriasis. *Arch Dermatol Res* 1994; 286: 455–461.
16. Berkers T, van Dijk L, Absalah S, van Smeden J, Bouwstra JA. Topically applied fatty acids are elongated before incorporation in the stratum corneum lipid matrix in compromised skin. *Exp Dermatol* 2017; 26: 36–43.
17. Kligman AM, Christophers E. Preparation of isolated sheets of

- human stratum corneum. *Arch Dermatol* 1963; 88: 702–705.
18. Bras W, Dolbnya IP, Detollenaere D, van Tol R, Malfois M, Greaves GN, et al. Recent experiments on a small-angle/wide-angle X-ray scattering beam line at the ESRF. *J Appl Cryst* 2003; 36: 791–794.
 19. Ponec M, Kempenaar J, Weerheim A. Lack of desquamation – the Achilles heel of the reconstructed epidermis. *Int J Cosmet Sci* 2002; 24: 263–272.
 20. Mojumdar EH, Helder RW, Gooris GS, Bouwstra JA. Monounsaturated fatty acids reduce the barrier of stratum corneum lipid membranes by enhancing the formation of a hexagonal lateral packing. *Langmuir* 2014; 30: 6534–6543.
 21. Mojumdar EH, Kariman Z, van KL, Gooris GS, Bouwstra JA. The role of ceramide chain length distribution on the barrier properties of the skin lipid membranes. *Biochim Biophys Acta* 2014; 1838: 2473–2483.
 22. Boiten W, Absalah S, Vreeken R, Bouwstra J, van Smeden J. Quantitative analysis of ceramides using a novel lipidomics approach with three dimensional response modelling. *Biochim Biophys Acta* 2016; 1861: 1652–1661.
 23. Kihara A. Synthesis and degradation pathways, functions, and pathology of ceramides and epidermal acylceramides. *Prog Lipid Res* 2016; 63: 50–69.
 24. Janssens M, van Smeden J, Gooris GS, Bras W, Portale G, Caspers PJ, et al. Increase in short-chain ceramides correlates with an altered lipid organization and decreased barrier function in atopic eczema patients. *J Lipid Res* 2012; 53: 2755–2766.
 25. Janssens M, Mulder AA, van Smeden J, Pilgram GS, Wolterbeek R, Lavrijsen AP, et al. Electron diffraction study of lipids in non-lesional stratum corneum of atopic eczema patients. *Biochim Biophys Acta* 2013; 1828: 1814–1821.
 26. Bouwstra JA, Nahmoed N, Groenink HW, Ponec M. Human skin equivalents are an excellent tool to study the effect of moisturizers on the water distribution in the stratum corneum. *Int J Cosmet Sci* 2012; 34: 560–566.
 27. Thakoersing VS, Gooris GS, Mulder A, Rietveld M, El Ghalbzouri A, Bouwstra JA. Unraveling barrier properties of three different in-house human skin equivalents. *Tissue Eng Part C Methods* 2012; 18: 1–11.
 28. el-Ghalbzouri A, Gibbs S, Lamme E, Van Blitterswijk CA, Ponec M. Effect of fibroblasts on epidermal regeneration. *Br J Dermatol* 2002; 147: 230–243.
 29. Stark HJ, Boehnke K, Mirancea N, Willhauck MJ, Pavesio A, Fusenig NE, et al. Epidermal homeostasis in long-term scaffold-enforced skin equivalents. *J Invest Dermatol Symp Proc* 2006; 11: 93–105.
 30. van Drongelen V, Danso MO, Mulder A, Mieremet A, van Smeden J, Bouwstra JA, et al. Barrier properties of an N/TERT-based human skin equivalent. *Tissue Eng Part A* 2014; 20: 3041–3049.
 31. van Drongelen V, Alloul-Ramdhani M, Danso MO, Mieremet A, Mulder A, van Smeden J, et al. Knock-down of filaggrin does not affect lipid organization and composition in stratum corneum of reconstructed human skin equivalents. *Exp Dermatol* 2013; 22: 807–812.